

Thermodynamic properties of $\text{Ba}_{1-x}\text{M}_x\text{Fe}_2\text{As}_2$ ($\text{M} = \text{La}$ and K)

J. K. Dong,¹ L. Ding,¹ H. Wang,¹ X. F. Wang,² T. Wu,² X. H. Chen,² and S. Y. Li^{1,*}

¹*Department of Physics, Surface Physics Laboratory (National Key Laboratory),
and Advanced Materials Laboratory, Fudan University, Shanghai 200433, P. R. China*

²*Hefei National Laboratory for Physical Science at Microscale and Department of Physics,
University of Science and Technology of China, Hefei, Anhui 230026, P. R. China*

(Dated: November 10, 2018)

The specific heat $C(T)$ of BaFe_2As_2 single crystal, electron-doped $\text{Ba}_{0.7}\text{La}_{0.3}\text{Fe}_2\text{As}_2$ and hole-doped $\text{Ba}_{0.5}\text{K}_{0.5}\text{Fe}_2\text{As}_2$ polycrystals were measured. For undoped BaFe_2As_2 single crystal, a very sharp specific heat peak was observed at 136 K. This is attributed to the structural and antiferromagnetic transitions occurring at the same temperature. $C(T)$ of the electron-doped non-superconducting $\text{Ba}_{0.7}\text{La}_{0.3}\text{Fe}_2\text{As}_2$ also shows a small peak at 120 K, indicating a similar but weaker structural/antiferromagnetic transition. For the hole-doped superconducting $\text{Ba}_{0.5}\text{K}_{0.5}\text{Fe}_2\text{As}_2$, a clear peak of C/T was observed at $T_c = 36$ K, which is the highest peak seen at superconducting transition for iron-based high- T_c superconductors so far. The electronic specific heat coefficient γ and Debye temperature Θ_D of these compounds were obtained from the low temperature data.

PACS numbers: 74.25.Bt, 74.25.Ha

The recent discovery of superconductivity with T_c as high as 55 K in iron-based $\text{LnO}_{1-x}\text{F}_x\text{FeAs}$ ($\text{Ln} = \text{La}, \text{Sm}, \text{Ce}, \text{Nd}, \text{Pr}, \text{Gd}, \text{Tb}, \text{Dy}$) has attracted great attention.^{1,2,3,4,5,6,7,8,9} It is believed that the FeAs layers are responsible for the high- T_c superconductivity and the LnO layers provide electron carriers through fluorine doping,^{1,2,3,4,5,6,7,8,9} by simply introducing oxygen vacancies,¹⁰ or by substituting Ln^{3+} with Th^{4+} .¹¹ This is very similar to the high- T_c cuprate superconductors. Since increasing the number of CuO_2 layers in one unit cell has been a promising way to elevate T_c for cuprates, many efforts have been put into searching superconductivity in iron-based compounds with multiple FeAs layers.

The ternary iron arsenide BaFe_2As_2 with the tetragonal ThCr_2Si_2 -type structure was first suggested by Rotter *et al.*¹² that it can serve as a parent compound for oxygen-free iron arsenide superconductors. Very soon, superconductivity with $T_c = 38$ K was indeed discovered in $\text{Ba}_{1-x}\text{K}_x\text{Fe}_2\text{As}_2$.¹³ In contrast to electron-doped $\text{LnO}_{1-x}\text{F}_x\text{FeAs}$, the carriers in $\text{Ba}_{1-x}\text{K}_x\text{Fe}_2\text{As}_2$ are holes introduced by potassium doping, which has been verified by Hall coefficient and thermoelectric power measurements.¹⁴ Later, superconductivity was also found in $\text{Sr}_{1-x}\text{M}_x\text{Fe}_2\text{As}_2$ ($\text{M} = \text{K}$ and Cs) and $\text{Ca}_{1-x}\text{Na}_x\text{Fe}_2\text{As}_2$ with $T_c \sim 38$ and 20 K, respectively.^{15,16,17} Interestingly, the electron-doped $\text{Ba}_{1-x}\text{La}_x\text{Fe}_2\text{As}_2$ shows no sign of superconductivity.¹⁴

For the parent compound BaFe_2As_2 , resistivity, specific heat, and susceptibility show clear anomaly near 140 K.^{12,18} Similar anomalies were also observed in SrFe_2As_2 and EuFe_2As_2 at relatively higher temperature near 200 K.^{15,19,20,21} Neutron scattering experiment has demonstrated that in BaFe_2As_2 there is a phase transition to a long-ranged antiferromagnetic state at 142 K where a first-order structural transition from tetragonal to orthorhombic symmetry also occurs.²² This is analogous to that in LaOFeAs compound, where structural and spin-

density-wave transitions were observed, but occurring at different temperatures, 155 K and 137 K respectively.²³ In both LnOFeAs and AFe_2As_2 ($\text{A} = \text{Ba}, \text{Sr}, \text{and Ca}$), antiferromagnetism gives way to superconductivity as electrons or holes are doped, indicating antiferromagnetic spin fluctuations may play an important role in these systems.

While the specific heat peak near 140 K was observed in BaFe_2As_2 polycrystalline sample,¹² it was absent from the $C(T)$ curve of the first reported BaFe_2As_2 single crystal.²⁴ The resistivity behavior of their single crystal²⁴ was also different from previous polycrystalline sample.¹³ These unusual resistivity and specific heat behaviors may result from the contamination of Sn flux in the crystal.²⁴ Therefore it is interesting to check the intrinsic specific heat behavior of BaFe_2As_2 single crystal with high purity. There are also no specific heat data for superconducting $\text{A}_{1-x}\text{M}_x\text{Fe}_2\text{As}_2$ ($\text{A} = \text{Ba}, \text{Sr}, \text{and Ca}$; $\text{M} = \text{K}, \text{Cs}, \text{and Na}$) compounds so far.

In this Brief Report, we present the first specific heat results of high quality BaFe_2As_2 single crystal, electron-doped $\text{Ba}_{0.7}\text{La}_{0.3}\text{Fe}_2\text{As}_2$ and hole-doped $\text{Ba}_{0.5}\text{K}_{0.5}\text{Fe}_2\text{As}_2$ polycrystals. Very sharp specific heat peak at 136 K was observed for our BaFe_2As_2 single crystal, 3 times higher than that in previous polycrystalline sample. A much smaller peak near 120 K was also observed for $\text{Ba}_{0.7}\text{La}_{0.3}\text{Fe}_2\text{As}_2$, indicating a weak structural/antiferromagnetic transition in this electron-doped sample. A clear peak of C/T shows up at $T_c = 36$ K for the hole-doped $\text{Ba}_{0.5}\text{K}_{0.5}\text{Fe}_2\text{As}_2$ superconducting sample. By fitting the low temperature data, the electronic specific heat coefficient γ and Debye temperature Θ_D of these compounds were obtained.

The single crystals of BaFe_2As_2 and polycrystalline samples with nominal composition $\text{Ba}_{0.7}\text{La}_{0.3}\text{Fe}_2\text{As}_2$ and $\text{Ba}_{0.5}\text{K}_{0.5}\text{Fe}_2\text{As}_2$ were prepared as in Ref. 14 and 18. By employing self-flux method (FeAs as flux), our BaFe_2As_2 single crystals are free of contamination from other ele-

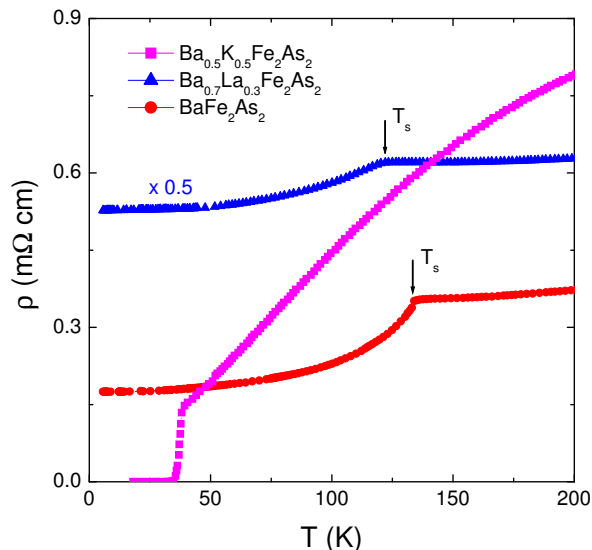


FIG. 1: (Color online) Resistivity of BaFe_2As_2 single crystal, electron-doped $\text{Ba}_{0.7}\text{La}_{0.3}\text{Fe}_2\text{As}_2$ and hole-doped $\text{Ba}_{0.5}\text{K}_{0.5}\text{Fe}_2\text{As}_2$ polycrystals. Arrows denote the structural and antiferromagnetic transitions occurring at the same temperature T_s .

ments. Resistivity were measured by the standard four-probe method. Specific heat measurements were performed in a Quantum Design physical property measurement system (PPMS) via the relaxation method. Magnetic field $H = 8$ T was applied for the $\text{Ba}_{0.5}\text{K}_{0.5}\text{Fe}_2\text{As}_2$ superconducting sample.

Fig. 1 shows the resistivity of BaFe_2As_2 single crystal, $\text{Ba}_{0.7}\text{La}_{0.3}\text{Fe}_2\text{As}_2$ and $\text{Ba}_{0.5}\text{K}_{0.5}\text{Fe}_2\text{As}_2$ polycrystals. Abrupt resistivity drop can be seen at $T_s = 134$ K for BaFe_2As_2 single crystal, consistent with previous reports.^{12,14} Similar resistivity drop was also observed for $\text{Ba}_{0.7}\text{La}_{0.3}\text{Fe}_2\text{As}_2$ sample, but less abrupt and shifting to lower temperature $T_s = 122$ K. No superconducting transition was observed at low temperature down to 5 K for the electron-doped $\text{Ba}_{0.7}\text{La}_{0.3}\text{Fe}_2\text{As}_2$, similar to previous $\text{Ba}_{0.85}\text{La}_{0.15}\text{Fe}_2\text{As}_2$ sample.¹⁴ The hole-doped $\text{Ba}_{0.5}\text{K}_{0.5}\text{Fe}_2\text{As}_2$ sample shows a sharp superconducting transition starting at 38 K and reaching zero resistivity at 34 K. We use the middle point of transition 36 K as its T_c .

The specific heat $C(T)$ of BaFe_2As_2 , $\text{Ba}_{0.7}\text{La}_{0.3}\text{Fe}_2\text{As}_2$ and $\text{Ba}_{0.5}\text{K}_{0.5}\text{Fe}_2\text{As}_2$ samples are shown in Fig. 2. For the BaFe_2As_2 single crystal, one can see a very sharp peak (enlarged in the inset) with $\Delta C \approx 130$ J / mol K, which is different from the first reported BaFe_2As_2 single crystal by Ni *et al.*,²⁴ and consistent with previous result on polycrystalline sample.¹² The height of specific heat peak in the insert of Fig. 2 is also 3 times higher than that in polycrystalline sample where $\Delta C \approx 35$ J / mol K.¹² This proves the high quality of our BaFe_2As_2 single crystal. It is believed that the use of self-flux method of growth gives the high purity of our samples, thus the intrinsic specific heat behavior of BaFe_2As_2 single crystal.

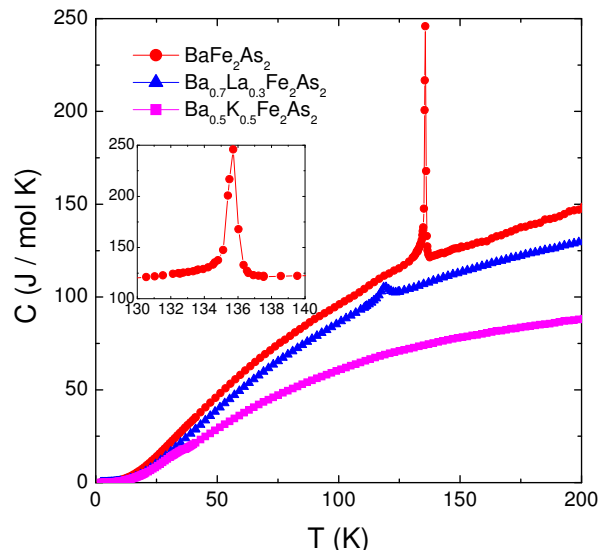


FIG. 2: (Color online) Specific heat of BaFe_2As_2 , $\text{Ba}_{0.7}\text{La}_{0.3}\text{Fe}_2\text{As}_2$ and $\text{Ba}_{0.5}\text{K}_{0.5}\text{Fe}_2\text{As}_2$ samples. The parent compound BaFe_2As_2 single crystal shows a very sharp peak at 136 K, enlarged in the insert. A small peak is also visible at 120 K for $\text{Ba}_{0.7}\text{La}_{0.3}\text{Fe}_2\text{As}_2$.

As found in SrFe_2As_2 ,¹⁹ the abrupt resistivity drop and sharp specific heat peak in Fig. 1 and 2 should be compatible with a first-order phase transition in BaFe_2As_2 . Neutron scattering experiment has demonstrated such first-order structural phase transition, accompanied by a long-range antiferromagnetic transition.²² The entropy connected with the transition $\Delta S \sim 1$ J / mol K is estimated from the area under the $C(T)$ peak in the insert of Fig. 2. This small value of ΔS is almost the same as that in SrFe_2As_2 .¹⁹

In Fig. 2, $C(T)$ of the electron-doped $\text{Ba}_{0.7}\text{La}_{0.3}\text{Fe}_2\text{As}_2$ sample also manifests a small peak at 120 K. This is consistent with the resistivity drop at 122 K in Fig. 1, indicating a similar but weaker structural/antiferromagnetic transition. No anomaly of $C(T)$ was observed above T_c for the hole-doped $\text{Ba}_{0.5}\text{K}_{0.5}\text{Fe}_2\text{As}_2$ sample. These results show that hole doping suppresses structural/antiferromagnetic transition more efficiently than electron doping in $\text{Ba}_{1-x}\text{M}_x\text{Fe}_2\text{As}_2$ system.

Fig. 3 plots C/T vs T for the superconducting $\text{Ba}_{0.5}\text{K}_{0.5}\text{Fe}_2\text{As}_2$ sample from 30 to 40 K in zero and $H = 8$ T magnetic fields. A clear peak shows up at $T_c = 36$ K and it is suppressed to lower temperature by 8 T field. Rough estimation gives the specific heat jump $\Delta C/T \approx 15$ mJ / mol K² at T_c in zero field. Previously, there was no visible anomaly on C/T near T_c for $\text{LaO}_{1-x}\text{F}_x\text{FeAs}$,^{25,26} and only a small kink was observed at T_c for $\text{SmO}_{1-x}\text{F}_x\text{FeAs}$.²⁷ To our knowledge, the C/T peak in Fig. 3 is the highest peak seen at the superconducting transition in iron-based high- T_c superconductors so far. This may be attributed to the better quality, or higher superfluid density of the $\text{Ba}_{0.5}\text{K}_{0.5}\text{Fe}_2\text{As}_2$ sample.

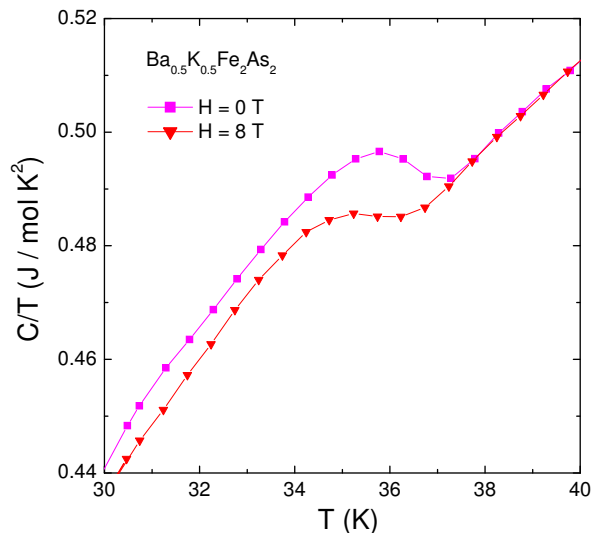


FIG. 3: (Color online) C/T vs T for $\text{Ba}_{0.5}\text{K}_{0.5}\text{Fe}_2\text{As}_2$ polycrystalline sample near $T_c = 36$ K in zero and $H = 8$ T magnetic fields. Rough estimation gives the specific heat jump $\Delta C/T \approx 15$ mJ / mol K^2 at T_c in zero field.

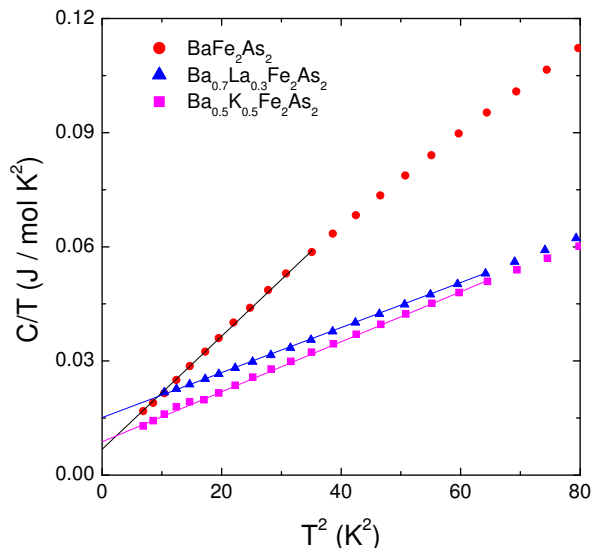


FIG. 4: (Color online) C/T vs T^2 for BaFe_2As_2 , $\text{Ba}_{0.7}\text{La}_{0.3}\text{Fe}_2\text{As}_2$ and $\text{Ba}_{0.5}\text{K}_{0.5}\text{Fe}_2\text{As}_2$ samples. The lines are linear fits at low temperature.

In Fig. 4, C/T vs T^2 is plotted for BaFe_2As_2 ,

$\text{Ba}_{0.7}\text{La}_{0.3}\text{Fe}_2\text{As}_2$ and $\text{Ba}_{0.5}\text{K}_{0.5}\text{Fe}_2\text{As}_2$ samples at low temperature. For BaFe_2As_2 single crystal, the data between 2 and 6 K can be linearly fitted to $C/T = \gamma + \beta T^2$, which gives the electronic specific heat coefficient $\gamma = 6.1 \pm 0.3$ mJ / mol K^2 and $\beta = 1.51 \pm 0.01$ mJ / mol K^4 . This value of γ is smaller than that obtained in polycrystal sample (16 mJ / mol K^2),¹² and much smaller than that of the first reported BaFe_2As_2 single crystal (37 mJ / mol K^2).²⁴ Using the equation $\beta = (12\pi^4 n k_B) / (5\Theta_D^3)$, where n is the number of atoms per formula unit, we estimate the Debye temperature $\Theta_D = 186$ K for BaFe_2As_2 single crystal.

For $\text{Ba}_{0.7}\text{La}_{0.3}\text{Fe}_2\text{As}_2$ and $\text{Ba}_{0.5}\text{K}_{0.5}\text{Fe}_2\text{As}_2$ samples, the data between 2 and 8 K can also be fitted as above, which gives $\gamma = 15.2 \pm 0.1$ mJ / mol K^2 , $\beta = 0.586 \pm 0.003$ mJ / mol K^4 , and $\gamma = 9.1 \pm 0.2$ mJ / mol K^2 , $\beta = 0.653 \pm 0.005$ mJ / mol K^4 , respectively. Comparing with the parent compound, electron doping seems to increase γ in the non-superconducting $\text{Ba}_{0.7}\text{La}_{0.3}\text{Fe}_2\text{As}_2$. The residual $\gamma = 9.1$ mJ / mol K^2 of the superconducting $\text{Ba}_{0.5}\text{K}_{0.5}\text{Fe}_2\text{As}_2$ sample suggests nodes in the superconducting gap. However, since these two samples are polycrystals, their values of γ may be not completely intrinsic. The Debye temperature of these two samples are estimated to be $\Theta_D = 254$ and 246 K, respectively.

In summary, we have studied the specific heat of high quality BaFe_2As_2 single crystal, electron-doped $\text{Ba}_{0.7}\text{La}_{0.3}\text{Fe}_2\text{As}_2$ and hole-doped $\text{Ba}_{0.5}\text{K}_{0.5}\text{Fe}_2\text{As}_2$ polycrystals. For BaFe_2As_2 single crystal, a very sharp specific heat peak at 136 K was observed, consistent with the polycrystal result. A small peak near 120 K was also observed for electron-doped $\text{Ba}_{0.7}\text{La}_{0.3}\text{Fe}_2\text{As}_2$, indicating a weak structural/antiferromagnetic transition. A clear peak of C/T can be seen at $T_c = 36$ K for the hole-doped $\text{Ba}_{0.5}\text{K}_{0.5}\text{Fe}_2\text{As}_2$ sample, which is the highest one among all iron-based high- T_c superconductors so far. By fitting the low temperature data, we obtain the electronic specific heat coefficient γ and Debye temperature Θ_D of these compounds.

This work is supported by the Natural Science Foundation of China, the Ministry of Science and Technology of China (973 project No: 2006CB601001 and National Basic Research Program No:2006CB922005), and STCSM of China.

* Electronic address: shiyan_li@fudan.edu.cn

¹ Yoichi Kamihara, Takumi Watanabe, Masahiro Hirano, and Hideo Hosono, *J. Am. Chem. Soc.* **130**, 3296 (2008).

² X. H. Chen, T. Wu, G. Wu, R. H. Liu, H. Chen, D. F. Fang, *Nature* **453**, 761 (2008).

³ Zhi-An Ren, Wei Lu, Jie Yang, Wei Yi, Xiao-Li Shen, Zheng-Cai Li, Guang-Can Che, Xiao-Li Dong, Li-Ling Sun, Fang Zhou, Zhong-Xian Zhao, *Chin. Phys. Lett.* **25**, 2215

(2008).

⁴ R. H. Liu, G. Wu, T. Wu, D. F. Fang, H. Chen, S. Y. Li, K. Liu, Y. L. Xie, X. F. Wang, R. L. Yang, C. He, D. L. Feng, X. H. Chen, arXiv:0804.2105.

⁵ G. F. Chen, Z. Li, D. Wu, G. Li, W. Z. Hu, J. Dong, P. Zheng, J. L. Luo, N. L. Wang, *Phys. Rev. Lett.* **100**, 247002 (2008).

- ⁶ Zhi-An Ren, Jie Yang, Wei Lu, Wei Yi, Xiao-Li Shen, Zheng-Cai Li, Guang-Can Che, Xiao-Li Dong, Li-Ling Sun, Fang Zhou, Zhong-Xian Zhao, *Europhys. Lett.* **82**, 57002 (2008).
- ⁷ Zhi-An Ren, Jie Yang, Wei Lu, Wei Yi, Guang-Can Che, Xiao-Li Dong, Li-Ling Sun, Zhong-Xian Zhao, arXiv:0803.4283.
- ⁸ Peng Cheng, Lei Fang, Huan Yang, Xiyu Zhu, Gang Mu, Huiqian Luo, Zhaosheng Wang, Hai-Hu Wen, *Science in China G* **51**, 719 (2008).
- ⁹ Jan-Willem G. Bos, George B. S. Penny, Jennifer A. Rodgers, Dmitry A. Sokolov, Andrew D. Huxley, and J. Paul Attfield, arXiv:0806.0926.
- ¹⁰ Zhi-An Ren, Guang-Can Che, Xiao-Li Dong, Jie Yang, Wei Lu, Wei Yi, Xiao-Li Shen, Zheng-Cai Li, Li-Ling Sun, Fang Zhou, Zhong-Xian Zhao, *Europhys. Lett.* **83**, 17002 (2008).
- ¹¹ Cao Wang, Linjun Li, Shun Chi, Zengwei Zhu, Zhi Ren, Yuke Li, Yuetao Wang, Xiao Lin, Yongkang Luo, Shuai Jiang, Xiangfan Xu, Guanghan Cao, Zhu'an Xu, arXiv:0804.4290.
- ¹² Marianne Rotter, Marcus Tegel, Dirk Johrendt, Inga Schellenberg, Wilfried Hermes, Rainer Pottgen, arXiv:0805.4021.
- ¹³ Marianne Rotter, Marcus Tegel and Dirk Johrendt, arXiv:0805.4630.
- ¹⁴ G. Wu, R. H. Liu, H. Chen, Y. J. Yan, T. Wu, Y. L. Xie, J. J. Ying, X. F. Wang, D. F. Fang and X. H. Chen, arXiv:0806.1459.
- ¹⁵ G. F. Chen, Z. Li, G. Li, W. Z. Hu, J. Dong, X. D. Zhang, P. Zheng, N. L. Wang, and J. L. Luo, arXiv:0806.1209.
- ¹⁶ Kalyan Sasmal, Bing Lv, Bernd Lorenz, Arnold M. Guloy, Feng Chen, Yu-Yi Xue and Ching-Wu Chu, arXiv:0806.1301.
- ¹⁷ G. Wu, H. Chen, T. Wu, Y. L. Xie, Y. J. Yan, R. H. Liu, X. F. Wang, J. J. Ying, and X. H. Chen, arXiv:0806.4279.
- ¹⁸ X. F. Wang, T. Wu, G. Wu, H. Chen, Y. L. Xie, J. J. Ying, Y. J. Yan, R. H. Liu, X. H. Chen, arXiv:0806.2452.
- ¹⁹ C. Krellner, N. Caroca-Canales, A. Jesche, H. Rosner, A. Ormeci, and C. Geibel, arXiv:0806.1043.
- ²⁰ Zhi Ren, Zengwei Zhu, Shuai Jiang, Xiangfan Xu, Qian Tao, Cao Wang, Chunmu Feng, Guanghan Cao, and Zhu'an Xu, arXiv:0806.2591.
- ²¹ H. S. Jeevan, Z. Hossain, C. Geibel, and P. Gegenwart, arXiv:0806.2876.
- ²² Q. Huang, Y. Qiu, Wei Bao, J.W. Lynn, M.A. Green, Y.C. Gasparovic, T. Wu, G. Wu, and X. H. Chen, arXiv:0806.2776.
- ²³ Clarina de la Cruz, Q. Huang, J. W. Lynn, Jiying Li, W. Ratcliff II, J. L. Zarestky, H. A. Mook, G. F. Chen, J. L. Luo, N. L. Wang, Pengcheng Dai, *Nature* **453**, 899 (2008).
- ²⁴ N. Ni, S. L. Bud'ko, A. Kreyssig, S. Nandi, G. E. Rustan, A. I. Goldman, S. Gupta, J. D. Corbett, A. Kracher, and P. C. Canfield, arXiv:0806.1874.
- ²⁵ Gang Mu, Xiyu Zhu, Lei Fang, Lei Shan, Cong Ren, and Hai-Hu Wen, *Chin. Phys. Lett.* **25**, 2221 (2008).
- ²⁶ Athena S. Sefat, Michael A. McGuire, Brian C. Sales, Rongying Jin, Jane Y. Howe, and David Mandrus, *Phys. Rev. B* **77**, 174503 (2008).
- ²⁷ L. Ding, C. He, J. K. Dong, T. Wu, R. H. Liu, X. H. Chen, and S. Y. Li, *Phys. Rev. B* **77**, 180510(R) (2008).